J. Membrane Biol. 116, 149–161 (1990)

The Journal of
Membrane Biology

Chloride and Potassium Channels in U937 Human Monocytes

Tomohiko Kanno* and Tamotsu Takishima
The First Department of Internal Medicine, Tohoku University School of Medicine, 1-1 Seiryo-machi, Aoba-ku, Sendai 980, Japan

Summary. Ionic channels in a human monocyte cell line (U937) were studied with the inside-out patch-clamp technique. A Ca^{2+}-activated K^+ channel and three Cl^--selective channels were observed. The Ca^{2+}-activated K^+ channel had an inward-rectifying current-voltage relationship with slope conductance of 28 pS, and was not dependent on membrane potential. Among the three Cl^- channels, an outward-rectifying 28-pS channel was most frequently observed. The permeability ratio (Cl^-/Na^+) was 4–5 and $CH_3SO_4^-$ was also permeant. The channel became less active with increasing polarizations in either direction, and was inactive beyond ±120 mV. The channel, observed as bursts, occasionally had rapid events within the bursts, suggesting the presence of another mode of kinetics. Diisothiocyanatostilbene-disulfonic acid (DIDS) blocked the channel reversibly in a dose-dependent manner. The second 328-pS Cl^- channel had a linear current-voltage relationship and permeability ratio (Cl^-/Na^+) of 5–6. This channel became less active with increasing polarizations and inactive beyond ±50 mV. DIDS blocked the channel irreversibly. The channel had multiple subconductance states. The third 15-pS Cl^- channel was least frequently observed and least voltage sensitive among the Cl^- channels. Intracellular Ca^{2+} or pH affected none of the three Cl^- channels. All three Cl^- channels had a latent period before being observed, suggesting inhibitory factor(s) present *in situ*. Activation of the cells with interferon-γ, interferon-αA or 12-O-tetradecanoylphorbol-13-acetate (TPA) caused no change in the properties of any of the channels.

Key Words Cl^- channel · K^+ channel · monocyte · macrophage · patch clamp

Introduction

Several ionic channels have been reported in monocytes/macrophages of various origins by the patch-clamp technique [19]. They are: delayed outward-rectifying K^+ channel [17, 24, 36, 39, 50], inward-rectifying K^+ channel [16, 17, 24, 30, 36], Ca^{2+}-activated K^+ channel [14, 16, 29, 36], Ca^{2+}-activated inward-rectifying K^+ channel [15], Fc-receptor linked nonselective cationic channel [32, 49], ATP-induced nonselective channel [6], and Cl^- channel with large conductance [24, 36, 41]. Monocytes/macrophages have many functions: nonspecific phagocytosis, antibody-dependent cellular cytotoxicity, antigen processing and presentation to lymphocytes, and secretion of immunological mediators, e.g., interleukin-1 (for review, *see* ref. [43]). Roles of ionic channels in such multifunctional cells, however, remain to be determined. We supposed that ionic channels may be expressed or repressed, or their characteristics may be modified through cellular activation and/or maturation. We thus studied ionic channels in U937, a human cell line with promonocytic characteristics [42], in which the functions of monocytes/macrophages can be inducible [25, 33, 34, 44]. We report here characteristics of four types of channels observed in inside-out patches. An abstract of this study has appeared [22].

Materials and Methods

Cell Culture and Cell Activation

The human monocytic cell line U937 [42] was maintained in RPMI-1640 supplemented with 10% heat-inactivated fetal bovine serum. When activated cells were examined, recombinant interferon-γ (rIFNγ; specific activity, 1×10^7 U/mg; used at 1000 U/ml), recombinant interferon-αA (rIFNαA; specific activity, 5.6×10^8 U/mg; used at 1000 U/ml) or 12-O-tetradecanoylphorbol-13-acetate (TPA, 10 ng/ml) was added to the medium on the first day and the effect on ionic channels was followed every day, up to the 4th day. Only TPA caused a marked morphological change in the cells. Recombinant IFNγ was generously provided by Shionogi Pharmaceutical, Osaka, Japan; and rIFNαA, by Nippon Roche Research Center, Kamakura, Japan. TPA was obtained from Sigma Chemical, St. Louis, MO. At the beginning of each experiment, cells were centrifuged and resuspended in an initial experimental solution so that concentrations of the fetal bovine serum and the activating agents were reduced to $<10^{-4}$ of the original concentrations.

* *Present address:* Pulmonary Branch, NHLBI, Building 10, Room 6N248, National Institutes of Health, Bethesda, MD 20892

Solutions

Exact compositions of pipette and bath solutions in each experiment are described in the figure legends. All solutions were buffered with either of the following (in mM) 5 N-2-hydroxyethylpiperazine-N'-2-ethanesulfonic acid (HEPES), 5 tris(hydroxymethyl) aminomethane (Tris), 5 N,N-*bis*[2-hydroxyethyl]-2-aminoethanesulfonic acid (BES), or 5 N-tris[hydroxymethyl]methyl-2-aminoethanesulfonic acid (TES). Because HEPES has been reported to block Cl^- channels in *Drosophila* neurons [48], we tested the four buffers, and confirmed that none of them, singly or in combination, affected the channel properties described here. In most experiments, solutions including 5 mM HEPES were adjusted with Tris to pH 7.2. When 5 mM Tris was used, we adjusted the pH with HCl. Solutions including 5 mM BES, 5 mM TES or, in some experiments, 5 or 20 mM HEPES were adjusted with NaOH. When effects of pH were examined, solutions with 5 mM BES were adjusted with NaOH to pH: 6.6, 6.9, 7.2, 7.5 or 7.8.

Desired concentrations of free calcium were achieved by mixing 4 mM ethyleneglycol-*bis*-(β-aminoethyl ether) N,N,N', N'-tetraacetic acid (EGTA) and varying amounts of $CaCl_2$ as follows. Initially, two kinds of stock solutions were prepared: Ca^{2+}-free EGTA solution adjusted roughly with Tris; and Ca^{2+}-EGTA solution made by mixing an equimolar amount of $CaCl_2$ and EGTA with twice the amount of NaOH or KOH. A calculated amount of the latter stock solution was added to experimental solutions, then the former stock solution was used to adjust the total EGTA concentration to 4 mM. Similarly, amounts of NaCl and KCl to be added were arranged to achieve desired total concentrations of the salts. To calculate the amount of $CaCl_2$-EGTA stock solution, the apparent binding constant of EGTA with calcium as determined by Harafuji and Ogawa [20] was used. Ionic strength of the solutions was not prescribed. Instead, iterative computations were carried out to approximate the value, with which the binding constants of EGTA and of the pH buffers were being corrected. Sometimes EGTA and $CaCl_2$ were not added to the K^+-free solutions, after we had confirmed that intracellular Ca^{2+} concentration had no effect on the Cl^- channel properties.

4,4'-diisothiocyanatostilbene-2,2'-disulfonic acid (DIDS) was obtained from Sigma.

Patch-Clamp Experiments

Patch-clamp experiments were carried out according to the standard method [19], using a List EPC-7 patch-clamp amplifier system (List Electronic, Darmstadt, FRG). All experiments were performed with inside-out or cell-attached patches at room temperature. All of the current traces shown in the figures were from inside-out patches. The recording chamber was composed of two parts; one for giga-seal formation and the other for solution change. The volume of the latter chamber was 70 μl and the bath solution was connected to a reference electrode via 150 mM or 1 M KCl/4% agar bridge. Liquid junction potentials which developed from solution changes were measured using a separate KCl-filled electrode and were used to correct membrane potentials. To change the bath solution, an infusion pump (Terumo, Tokyo, Japan) was used at a rate of 13 ml/min until over 30 times the chamber volume had been perfused. Pipettes were usually coated with Sylgard (Corning, Midland, MI), and fire polished. Pipette resistances ranged from 2 to 5 MΩ. Seal resistances ranged from 2 to 70 GΩ. Current recordings were stored on FM tape (Sony Magnescale, Tokyo; frequency response, DC to 5 kHz), and low-pass filtered (NF Circuit Design Block, Yokohama, 8-pole Bessel; 48 dB/octave) during playing back at normal or reduced tape speed. Data were analyzed with a computer system (7T17, NEC-Sanei, Tokyo, Japan). Current traces appearing in the figures were filtered for display purposes, that is, with different settings from those for the corresponding data analysis.

Data Analysis

Stability Plots

Data on tape were played back at one-tenth of the recorded speed, low-pass filtered at 250 Hz, then sampled every 400 μsec. Open and shut intervals were measured with the 50% threshold criterion [9]. Test pulses of various durations were used to calibrate the real intervals and to check the frequency response of the system. Pulses with durations over 800 μsec maintained their shape. Those with durations between 200 and 400 μsec crossed the 50% threshold, but were distorted in shape. Stability plots as described by Blatz and Magleby [3] were made to test for possible moding behavior. Durations of successive open and shut intervals were averaged separately by 25 or 50 events, and the mean open and shut intervals were plotted semilogarithmically against interval number.

Open Probability

Open probability is equal to the sum of open intervals measured in a given period, divided by the duration of the period. When more than one channel of the same type was present in a patch, total open intervals in each unitary level were added and divided by the product of time multiplied by the number of channels included in the patch.

Results

In unstimulated U937 human monocytes, we observed a Ca^{2+}-activated K^+ channel and three Cl^--selective channels. The Cl^- channels had different conductances: we refer to them as the large, intermediate and small Cl^- channels.

Intermediate Cl^- Channel and K^+ Channel

Figure 1 shows current traces from an inside-out patch containing the K^+ channel and the intermediate Cl^- channel. With 37.5 mM K^+/150 mM Cl^- in the pipette and 112.5 mM K^+/150 mM Cl^- in the bath, the expected reversal potentials for K^+ and Cl^- channels were -28 and 0 mV, respectively. Immediately after excising the patch (with 3 μM bath Ca^{2+} concentration), current was observed through only the K^+ channel (Fig. 1*a*). The current reversed near -30 mV. The K^+ current disappeared when

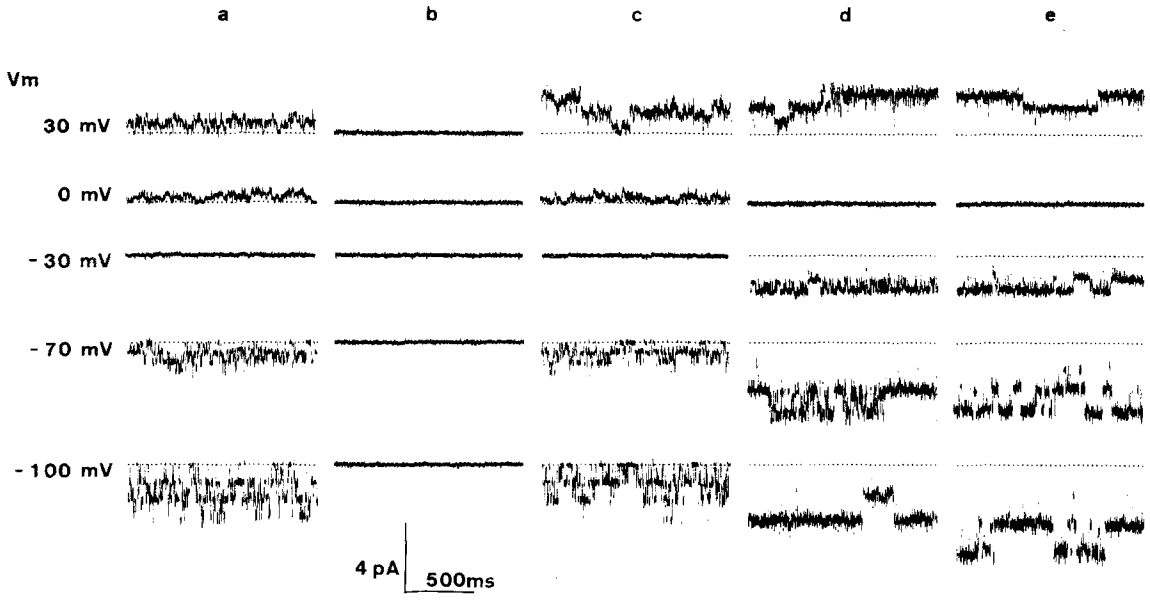

Fig. 1. Current traces recorded in an inside-out patch including both K^+ channels and intermediate Cl^- channels. Membrane potentials are indicated at the left. The traces were obtained successively: (*a*) immediately after excising the inside-out patch; (*b*) after 7 min; (*c*) after 10 min; (*d*) after 20 min; and (*e*) after 38 min. Free Ca^{2+} concentrations of the bath solutions were 3 μM (*a* and *c*), and 1 nM (*b*, *d* and *e*). The pipette solution contained 112.5 mM NaCl and 37.5 mM KCl. The bath solutions contained 37.5 mM NaCl and 112.5 mM KCl. Calculated equilibrium potentials for K^+ ion and Cl^- ion were −28 and 0 mV, respectively. All solutions contained 4 mM EGTA and 5 mM HEPES. pH = 7.2. The dotted lines represent current levels with all channels closed. The current was filtered at 300 Hz (−3 dB)

the intracellular Ca^{2+} concentration was reduced to 1 nM (Fig. 1*b*), and reappeared when the Ca^{2+} concentration was elevated again to 3 μM (Fig. 1*c*). Thus the K^+ channel current required intracellular Ca^{2+}. The open probability of the K^+ channel was not voltage dependent.

In contrast to the K^+ channel, current through the intermediate Cl^- channel did not appear until some time after the patch had been excised, either in high (3 μM) or low (1 nM) Ca^{2+} (Fig. 1*a* and *b*). In Fig. 1*c*, about 10 min after excising the patch, the Cl^- channel current appeared only at positive potentials. While the K^+ channel was deactivated by reducing the Ca^{2+} concentration to 1 nM, the Cl^- channel remained active (Fig. 1*d*: 20 min after excising the patch). The Cl^- channel was more active in Fig. 1*d* than in Fig. 1*c*, because current fluctuations were observed also at negative potentials in Fig. 1*d*. The Cl^- channel became more active 18 min later (Fig. 1*e*) and was stable thereafter. The time needed for such initial activation varied approximately from 10 sec to 30 min. Because the bath solutions in Fig. 1*b*, *d* and *e* contained the same components, the apparent activation of the channel may be due to breakdown or washout of factor(s) inhibitory to the intermediate Cl^- channel. Another observation that the Cl^- channel did not appear in cell-attached patches also suggests the presence of the factor(s) inhibitory to the channel *in situ*.

Figure 2 shows the *I-V* relationships of the K^+ channel. Each point is a mean value obtained from different patches, and the standard errors of the mean are indicated only when the values are larger than the size of symbols. The curve for symmetrical 150 mM KCl solutions (n = 6) showed inward-going rectification, and the slope conductance was 28 pS between −40 and −100 mV (Fig. 2*a*). When the bath solutions were replaced with solutions containing 450 mM KCl, the reversal potential was −27 mV (Fig. 2*b*). With 112.5 mM Na^+/37.5 mM K^+/150 mM Cl^- in the pipette and 37.5 mM Na^+/112.5 mM K^+/150 mM Cl^- in the bath, the reversal potential was also −27 mV (Fig. 2*c*). These experiments show that the K^+ channel is highly selective to K^+ ($P_K : P_{Na} : P_{Cl}$ = 70 : 1 : 1) as calculated from the Goldman-Hodgkin-Katz equation. Other observations also support the K^+ selectivity of the channel. Inward current through the K^+ channel was no longer observed when K^+ in the pipette solution was replaced by Na^+ (Fig. 2*d*), and conversely, outward current was no longer observed when K^+ in the bath solution was replaced by Na^+ (Fig. 2*e*).

Figure 3 shows the *I-V* relationships of the intermediate Cl^- channel. A curve for symmetrical 150 mM NaCl solutions (n = 66) is shown in Fig. 3*a*. The

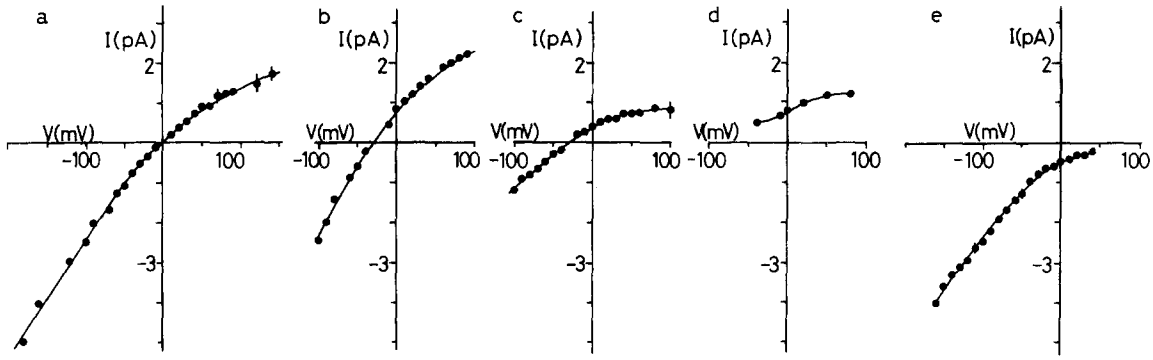

Fig. 2. Current-voltage relationships of the K^+ channel. Ionic compositions (pipette/bath) were as follows: (*a*) 150 mM KCl/150 mM KCl ($n = 6$), (*b*) 150 mM KCl/450 mM KCl ($n = 6$), (*c*) 37.5 mM KCl + 112.5 mM NaCl/112.5 mM KCl + 37.5 mM NaCl ($n = 24$), (*d*) 150 mM NaCl/150 mM KCl ($n = 4$), and (*e*) 150 mM KCl/150 mM NaCl ($n = 6$). All the solutions contained 4 mM EGTA, 5 mM HEPES, and 1 mM free Mg^{2+}. Free Ca^{2+} concentrations of the bath solutions were 0.1–30 μM. pH = 7.2. Association constants of $[MgEGTA^{2-}]/[Mg^{2+}][EGTA^{4-}] = 1.62 \times 10^5\ M^{-1}$ and $[MgHEGTA^-]/[Mg^{2+}][HEGTA^{3-}] = 2.34 \times 10^3\ M^{-1}$ were used to calculate required amounts of $MgCl_2$. The standard errors of the mean are shown by bars when they are larger than the symbol. Points at −160 and −180 mV in *a* were obtained with only one patch

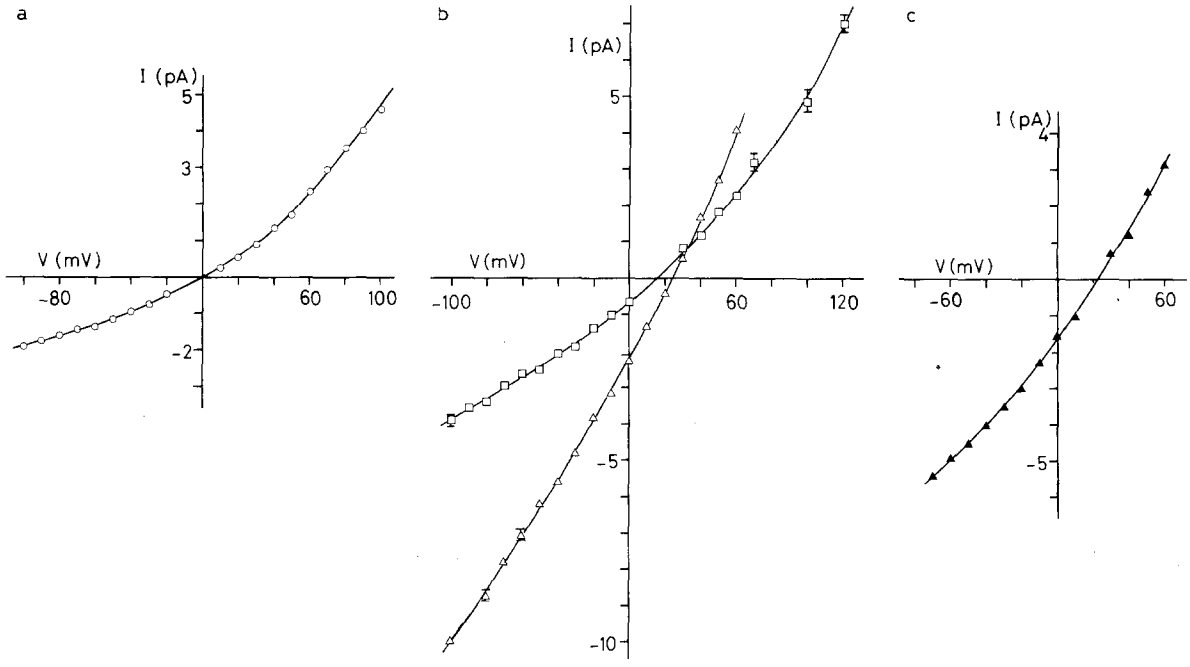

Fig. 3. (*a* and *b*) Current-voltage relationships of the intermediate Cl^- channel obtained with symmetrical 150 mM NaCl solutions (○, $n = 66$) (*a*), and with solutions giving threefold (□, $n = 20$) and fivefold (△, $n = 7$) concentration gradients (*b*). The pipette solutions contained 150 mM NaCl; the bath solutions contained 150 mM NaCl (○), 450 mM NaCl (□) or 750 mM NaCl (△). All the solutions contained 5 mM HEPES, adjusted with Tris to pH 7.2. The standard errors of the mean are shown by bars when they are larger than the symbols. (*c*) A current-voltage relationship of the intermediate Cl^- channel with a pipette solution of 150 mM NaCl and a bath solution of 750 mM $NaCH_3SO_4$

curve showed outward-going rectification: the chord conductance between 0 and 100 mV was 47 pS; the slope conductance around 0 mV was 28 pS. We examined the *I-V* curves with symmetrical 150 mM KCl solutions and with solutions described in Fig. 1, and they were almost identical to the curve shown in Fig. 3*a*. With the pipette solution containing 150 mM NaCl and the bath solution containing 450 or 750 mM NaCl, the reversal potentials were 16 mV ($n = 20$) and 24 mV ($n = 7$), respectively (Fig.

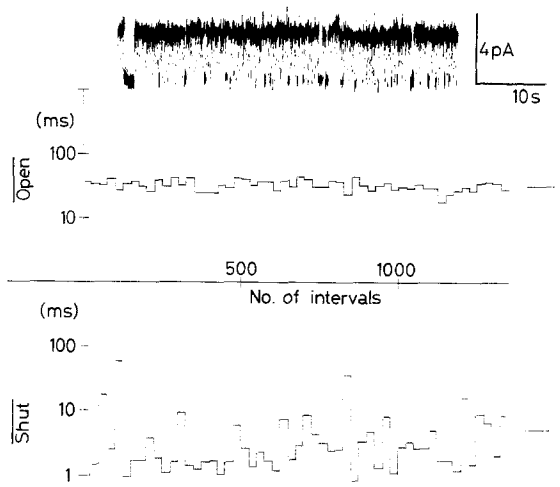

Fig. 4. Stability plots for open and shut intervals of the intermediate Cl^- channel. Averaged durations of 25 successive open or shut intervals are plotted semilogarithmically against interval number. The bars on the right side indicate the overall means of the intervals: 32.6 msec for the open intervals, 5.2 msec for the shut intervals. The corresponding current trace, filtered at 180 Hz (−3 dB), is shown in the upper part. The outward current direction is upward. Both the pipette and the bath solutions contained 140 mM NaCl and 5 mM Tris; pH was adjusted to 7.2 with HCl. The membrane potential was 60 mV

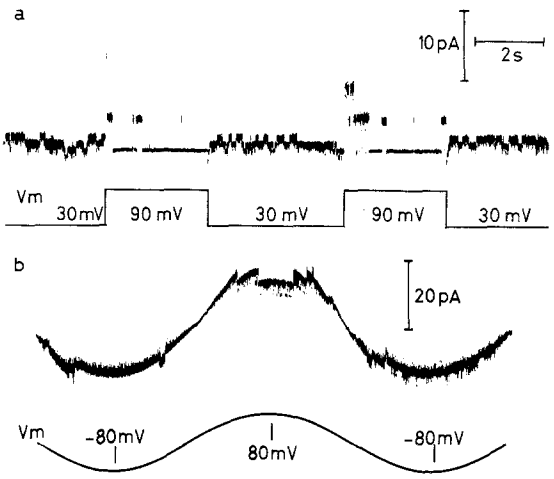

Fig. 5. Voltage dependence of the intermediate Cl^- channel. (*a*) Current response (upper trace) to voltage jumps (lower trace) is shown. The membrane potential was changed suddenly between 30 and 90 mV. The outward current direction is upward. The current was filtered at 900 Hz (−3 dB). The pipette and the bath solutions contained 150 mM KCl, 5 mM HEPES and 4 mM EGTA; pH was adjusted to 7.2 with Tris; free Ca^{2+} was less than 1 nM. (*b*) Current response (upper trace) to sinusoidal command voltage (lower trace). The sinusoidal voltage of 0.1 Hz was made between 80 and −80 mV. The current was filtered at 900 Hz (−3 dB). The pipette solution contained 150 mM NaCl, 5 mM HEPES and 4 mM EGTA, pH was adjusted to 7.2 with Tris; free Ca^{2+} was 3 μM. The bath solution contained 450 mM NaCl, 5 mM HEPES and 4 mM EGTA, pH was adjusted to 7.2 with Tris; free Ca^{2+} was 3 μM

3*b*). According to the Goldman-Hodgkin-Katz equation, permeability ratios for Cl^- to Na^+ corresponding to these values were 4.2 and 4.8, respectively. With 150 mM KCl in the pipette and 450 mM KCl in the bath, the reversal potential was also 16 mV ($n = 4$). Thus, the channel is more permeable to Cl^- than to either Na^+ or K^+. Permeability to $CH_3SO_4^-$ was examined in two patches. With 750 mM $NaCH_3SO_4$ in the bath and 150 mM NaCl in the pipette, reversal potential was 23 mV. The ratio of the current amplitude compared to that with 750 mM NaCl in the bath was about 0.7 (Fig. 3*c*). Although $CH_3SO_4^-$ seemed less permeant than Cl^- in conductance, it was not an impermeant ion through the intermediate Cl^- channel.

The intermediate Cl^- channel appeared in bursts rather than as isolated events. Figure 4 shows a representative trace of bursting current recorded from a patch with only one channel. Stability plots are shown below the current trace. The overall mean of open intervals (32.6 msec) was larger than that of shut intervals (5.2 msec). Moving mean durations of consecutive 25 open intervals fluctuated much less than those of shut intervals.

Most patches included two to four of the intermediate Cl^- channels. The Cl^- channels became less active with increasing membrane polarization in either direction. Figure 5 shows the representative traces. In Fig. 5*a*, current response to voltage jumps between 30 and 90 mV is shown. Inactivation at 90 mV occurred within a few seconds; reactivation at 30 mV occurred more quickly. To examine the voltage dependence through a range of membrane potentials, a sinusoidal command voltage of about 0.1 Hz was applied to the patch (Fig. 5*b*). The channels tended to close with increasing membrane polarization. In most patches, the channel was more active at positive potentials than at negative potentials when compared at the same degree of polarization. Current steps were rarely observed beyond 120 mV in either direction.

Sudden changes in kinetic behavior were occasionally observed (Fig. 6). As shown in the lower trace of Fig. 6*a*, the duration of open intervals suddenly changed. In this patch, simultaneous opening of more than one channel was never observed. The amplitude histogram is shown in Fig. 6*b*. Stability plots were made in order to look for possible moding behavior. In Fig. 6*c*, moving mean durations of consecutive groups of 50 open intervals were less than 10 msec for many intervals, then suddenly shifted to values more than 10 times longer which were maintained for hundreds of intervals. Corre-

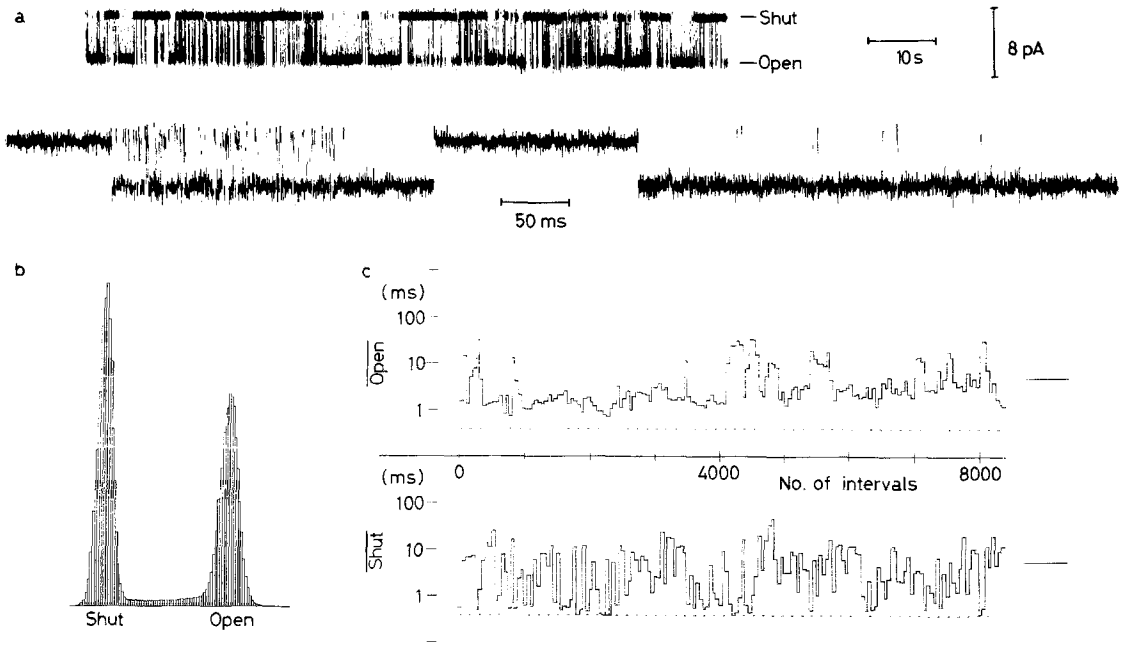

Fig. 6. (*a*) Current through the intermediate Cl^- channel is shown with low time resolution in the upper trace (filtered at 360 Hz), part of which is shown expanded in the lower trace (filtered at 3 kHz). The inward current direction is downward. The pipette solution contained 150 mM NaCl and 5 mM Tris; pH was adjusted to 7.2 with HCl. The bath solution contained 750 mM NaCl and 5 mM Tris; pH was adjusted to 7.2 with HCl. The membrane potential was −40 mV. (*b*) Amplitude histogram of the current record shown in *a*. The horizontal coordinate represents relative current amplitude and the vertical coordinate relative number of the events. (*c*) The stability plots for the open and shut intervals in the record shown in *a*. Averages of durations of 50 successive intervals are plotted semilogarithmically against interval number. The overall means are shown as bars in the right-hand side: 5.0 msec for the open intervals, 5.6 msec for the shut intervals. Limit of resolution in our system is shown with the dotted lines, under which individual intervals may be underestimated

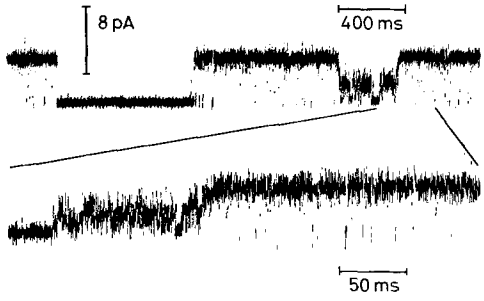

Fig. 7. Apparent subconductance states of the intermediate Cl^- channel. Part of the upper trace is shown expanded in the lower trace. V_m = 90 mV; the outward current direction is upward. The pipette solution contained 150 mM NaCl, 5 mM HEPES and 4 mM EGTA, pH was adjusted to 7.2 with Tris; free Ca^{2+} was 3 μM. The bath solution contained 450 mM NaCl, 5 mM HEPES and 4 mM EGTA; pH was adjusted to 7.2 with Tris; free Ca^{2+} was 1 nM

sponding changes in the mean shut intervals were not apparent. A sudden change in mean interval durations indicates a shift to another mode of kinetics [3, 31]. Thus, the stability plots suggest at least two modes are present in the intermediate Cl^- channel. As has been shown in Fig. 4 and from observations in many other patches, open intervals were usually of the order of tens of milliseconds. The longer mode in the patch shown in Fig. 6, thus, corresponds to the usual one, and the shorter mode is to be interpreted as unusually brief. We could easily detect the appearance of the briefer mode because its bursts were rapid compared to the usual bursts, as in Fig. 6*a*. The mode appeared in less than a tenth of all patches examined, and only occasionally appeared even in such patches. We never observed a patch with only the brief mode.

An apparent subconductance state(s) was occasionally observed (Fig. 7). The state(s) in the intermediate Cl^- channel was most frequently observed when polarization of the membrane was large enough to reduce the open probability of the channel. The state(s) was almost always accompanied by rapid openings and closings as shown in the left-hand part of the lower trace.

We studied regulatory effects of intracellular Ca^{2+} and pH on the intermediate Cl^- channel. Free calcium concentrations in the bath solutions were 1 nM, 100 nM, 3 μM and 30 μM; and pH values were

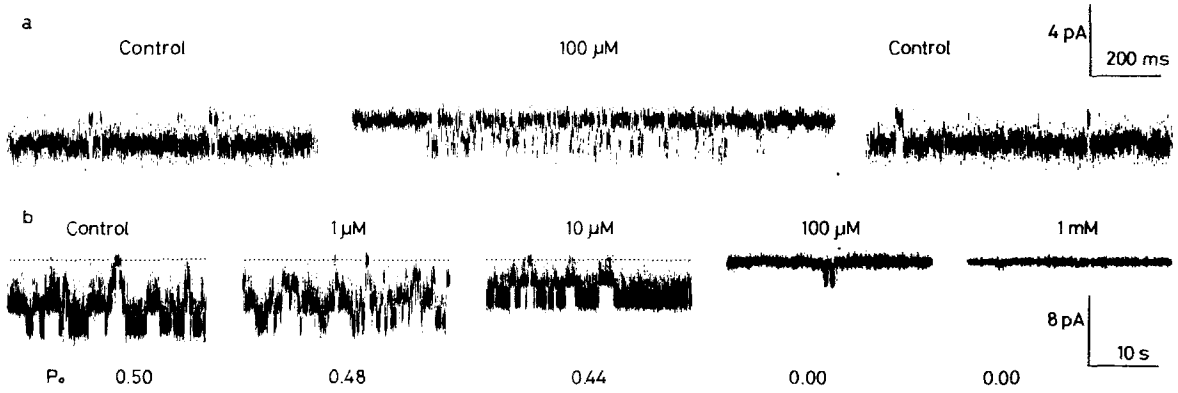

Fig. 8. Effect of DIDS on the intermediate Cl^- channel. The pipette solution contained 150 mM NaCl, 5 mM HEPES and 4 mM EGTA; pH was adjusted to 7.2 with Tirs; free Ca^{2+} was calculated to be less than 1 nM. The bath solution contained 450 mM NaCl, 5 mM HEPES and 4 mM EGTA; pH was adjusted to 7.2 with Tris; free Ca^{2+} was calculated to be less than 1 nM. The concentrations of DIDS are indicated above the current traces. The control solution contained no DIDS. The membrane potential was −30 mV. (*a*) Current traces from a patch with only one intermediate Cl^- channel. After the control recording, the bath solution including 100 μM DIDS was perfused, followed by washout with the control solution. The inward current direction is downward. The trace was filtered at 1.8 kHz (−3 dB). (*b*) Current traces from another patch which contained three intermediate Cl^- channels. The dotted lines represent the current level with no channels open. The solutions including increasing doses of DIDS (from 1 μM to 1 mM) were successively perfused. Open probabilities (P_o) are described under the traces. Filtered at 160 Hz (−3 dB)

6.6, 6.9, 7.2, 7.5 and 7.8. Neither changes in Ca^{2+} concentrations nor pH caused any reproducible change in the open probability or the moding behavior of the channel.

Because pH buffers such as HEPES have been reported to block Cl^- channels in *Drosophila* neurons [48], the effect of several buffers on the intermediate Cl^- channel activity was also examined. They were HEPES (5 or 20 mM), Tris (5 mM), BES (5 mM), TES (5 mM) and EGTA (5 or 20 mM). A control solution contained 150 mM NaCl and 5 mM Tris, and was adjusted to pH 7.2 with HCl. Varying the buffers, solely or in combination, caused no change in the moding behavior or appearance of the subconductance states.

We examined the effect of DIDS, a widely used Cl^- channel blocker, on the intermediate Cl^- channel activity in 10 patches. The blockade was flickery, reversible (Fig. 8*a*), and dose dependent (Fig. 8*b*). As shown in Fig. 8*b*, the open probability remained similar to the control value until the dose was over 10 μM; it was reduced to near zero with 100 μM DIDS.

Large Cl^- Channel

Like the intermediate Cl^- channel, the large Cl^- channel was not immediately observed upon excision of the patch. The latent time was longer than that for the intermediate Cl^- channel present in the same patches. Voltage dependence of the large Cl^- channel was more prominent than that of the intermediate Cl^- channel. The large Cl^- channel became less active with increasing polarization in either direction, and was rarely observed at stationary voltages more than 50 mV or less than −50 mV. The voltage dependence was most clearly demonstrated with voltage jumps, as shown in Fig. 9*a*. The large Cl^- channel appeared as bursts, which became inactivated more quickly with larger voltage jumps in either direction.

Figure 9*b* shows the *I-V* relationship of the large Cl^- channel (obtained with 50 patches). With symmetrical 150 mM NaCl solutions, the relationship was linear; the conductance was 328 pS. The reversal potentials were 18 mV with 450 mM NaCl in the bath ($n = 4$), and 27 mV with 750 mM NaCl in the bath ($n = 6$). According to the Goldman-Hodgkin-Katz equation, permeability ratios for Cl^- to Na^+ were 5.2 and 6.4, respectively.

The large Cl^- channel frequently showed subconductance states. Consecutive current traces are shown in Fig. 10*a*. The current fluctuated not only between the fully open and shut states, but also stayed at intermediate levels between the two states, which is prominent in the second and third traces. Some sections, as shown expanded in Fig. 10*b,i*, were well resolved as subconductance states; while others, as shown in Fig. 10*b,ii*, were not. The intermediate current level (especially in the third trace of *a*) showed an apparent increase in the noise level as compared to the fully open and shut states. The apparent increase in noise might represent

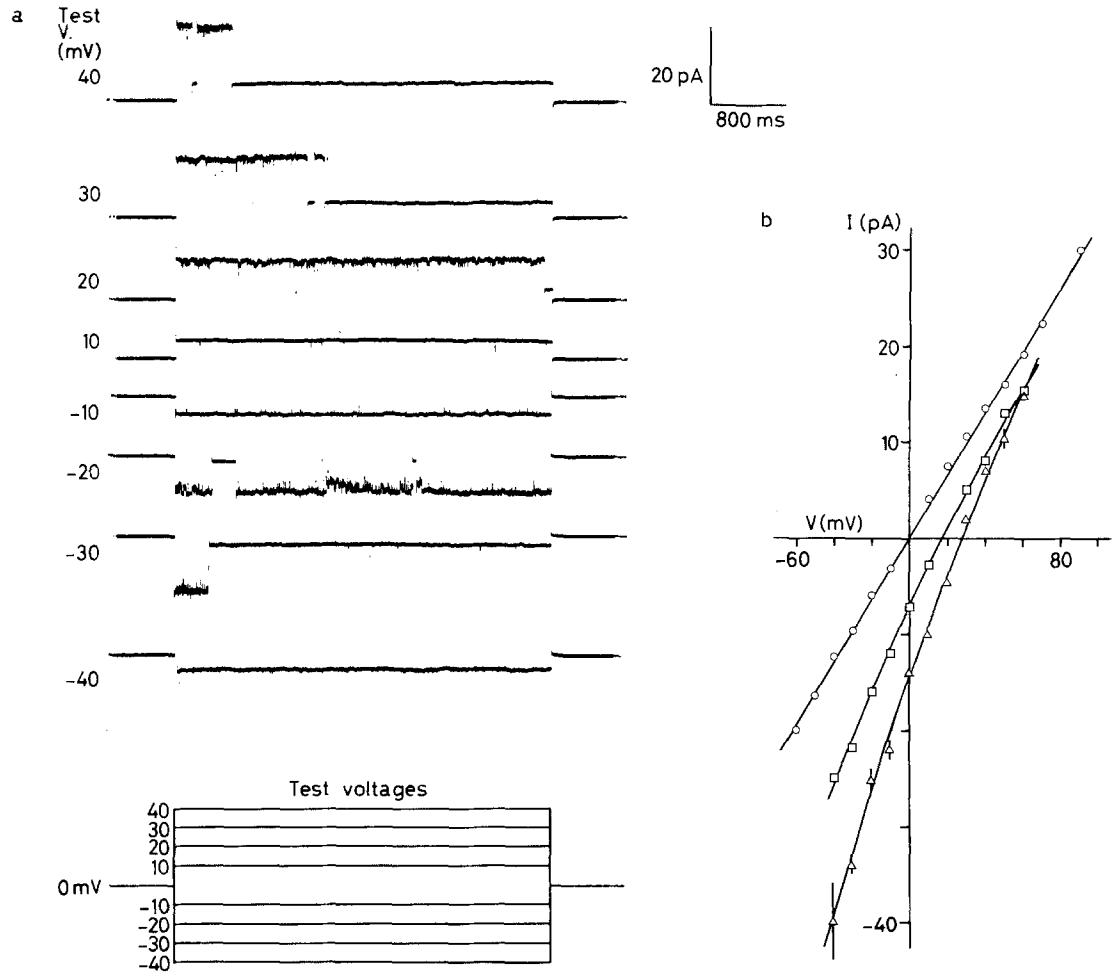

Fig. 9. Current traces and current-voltage relationships of the large Cl^- channel. (*a*) Current traces obtained with voltage jumps from 0 mV. The test voltages are indicated at the left side. The pipette and the bath solutions contained 150 mM NaCl, 5 mM HEPES and 4 mM EGTA; pH was adjusted to 7.2 with Tris; free Ca^{2+} was less than 1 nM. The record was filtered at 900 Hz (−3 dB). (*b*) Current-voltage relationships obtained with symmetrical 150 mM NaCl solutions (○) (n = 50) and solutions giving threefold (□) (n = 4) and fivefold (△) (n = 6) concentration gradients. The pipette solutions contained 150 mM NaCl, 5 mM HEPES and 4 mM EGTA; pH was adjusted to 7.2 with Tris; free Ca^{2+} was 1 nM to 30 μM. The bath solutions contained: 150 mM NaCl (○), 450 mM NaCl (□) or 750 mM NaCl (△); 5 mM HEPES; pH adjusted to 7.2 with Tris; 4 mM EGTA; free Ca^{2+} was 1 nM to 30 μM. Standard errors of the mean are shown by bars when they are larger than the symbols

rapid current fluctuation between two subconductance states rather than a single, noisy subconductance level. Because of the increased noise of the subconductance current levels, we filtered the record at 6 Hz in order to see the averaged subconductance states. The result is shown in Fig. 10*c*; the apparent subconductance levels, which were possibly modified by rapid kinetics, were composed of at least six levels.

With HEPES, Tris, TES or BES as a pH buffer, similar subconductance states were observed with similar frequency. The subconductance states, thus, were not due to the effect of the buffers, an effect which has been reported in *Drosophila* neurons [48]. Neither free Ca^{2+} concentration nor pH of the bath solution affected the open probability of the large Cl^- channel or the frequency of the subconductance states.

Sections of current traces which did not include subconductance states did not have unusually fast bursts, suggesting absence of the moding behavior in the large Cl^- channel. The stability plots of the large Cl^- channel showed little fluctuation in the open intervals (Fig. 11).

The effect of DIDS on the large Cl^- channel was examined in six patches. Figure 12 shows current traces obtained with a voltage-jump experiment. DIDS (100 μM) caused flickery block at 10 and 20 mV. At 30 mV, early inactivation was followed by very short openings. The mean of open

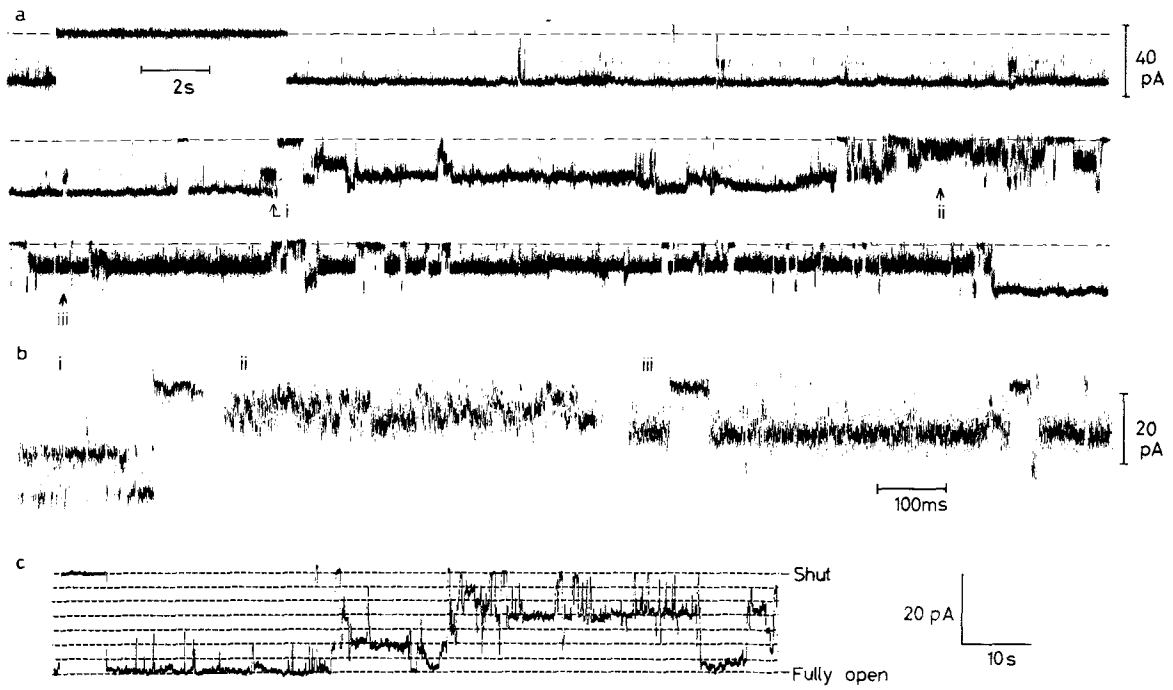

Fig. 10. Current traces of the large Cl^- channel showing subconductance levels. The pipette solution contained 150 mM NaCl and 5 mM Tris; pH was adjusted to 7.2 with HCl. The bath solution contained 750 mM NaCl and 5 mM Tris; pH was adjusted to 7.2 with HCl. $V_m = -20$ mV. (*a*) Consecutive current traces filtered at 1.8 kHz (−3 dB). The dotted line represents the level with the channel shut. (*b*) Parts of the traces in *a*, indicated by arrows as *i*, *ii* and *iii*, are shown with higher time resolution of 4.8 kHz (−3 dB). Vertical scales represent 40 pS (*a*), and 20 pS (*b* and *c*). (*c*) The record shown in *a* was filtered further at 6 Hz (−3 dB). The dotted lines represent the apparent subconductance levels

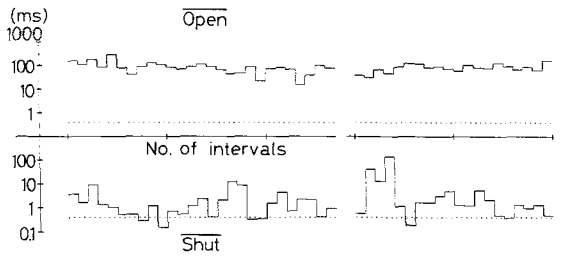

Fig. 11. Stability plots for open and shut intervals of the large Cl^- channel. Averaged durations of 50 successive open or shut intervals are plotted semilogarithmically against interval number. Plots are interrupted to avoid a section corresponding to the subconductance states. One division on the horizontal coordinate corresponds to 500 intervals. Limit of resolution is shown with the dotted lines, under which individual intervals may be underestimated. The pipette solution contained 150 mM NaCl and 5 mM Tris; pH was adjusted to 7.2 with HCl. The bath solution contained 750 mM NaCl and 5 mM Tris; pH was adjusted to 7.2 with HCl. $V_m = -20$ mV

intervals at 20 mV was 82.6 msec with control solution and 8.1 msec with 100 μM DIDS. The mean of shut intervals at 20 mV was 0.7 msec with control solution and 0.6 msec with 100 μM DIDS. With 1 mM DIDS, clearly resolved current steps were not observed. The effect of DIDS on the large Cl^- channel was irreversible.

Small Cl^- Channel

The small Cl^- channel was observed in 35 out of 396 patches, least frequently among the three Cl^- channels. In patches including both the small and the intermediate Cl^- channels, the small Cl^- channel was less voltage sensitive. Current traces from a patch including both the intermediate and small Cl^- channels are shown in Fig. 13*a*. The pipette solution contained 150 mM NaCl, and the bath solution contained 450 mM NaCl. At 120 mV, only the small Cl^- channels were observed, and transient subconductance state(s) also appeared. At −30 and −90 mV, the smaller steps correspond to the small Cl^- channel, and the larger steps correspond to the intermediate Cl^- channel. Figure 13*b* shows the *I-V* relationships of the small Cl^- channel with symmetrical solutions ($n = 35$) and with solutions giving a threefold Cl^- gradient ($n = 2$). The curve with symmetrical 150 mM NaCl solutions showed outward-going rectification, especially with negative voltages, and the slope conductance around 0 mV was 15 pS.

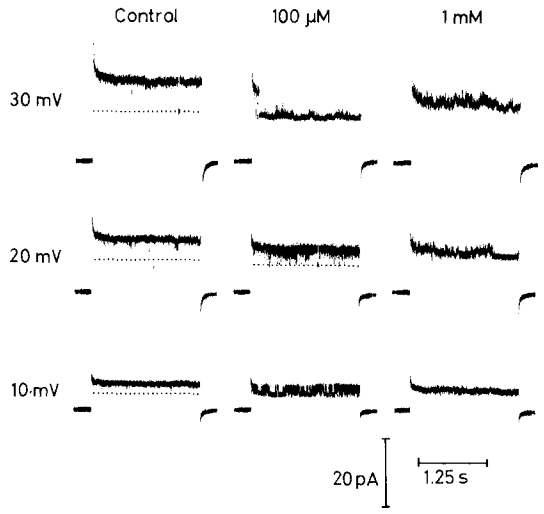

Fig. 12. Effect of DIDS on the large Cl^- channel. Voltage jumps from a holding voltage (0 mV) to test voltages of 10, 20 and 30 mV were performed. The dotted lines represent current level with no channel open. Both the pipette and bath solutions contained 150 mM NaCl and 5 mM BES; pH was adjusted to 7.2 with NaOH. The control solution without DIDS was replaced successively by the solutions containing 100 μM and 1 mM DIDS. The current traces were filtered at 1.3 kHz (−3 dB)

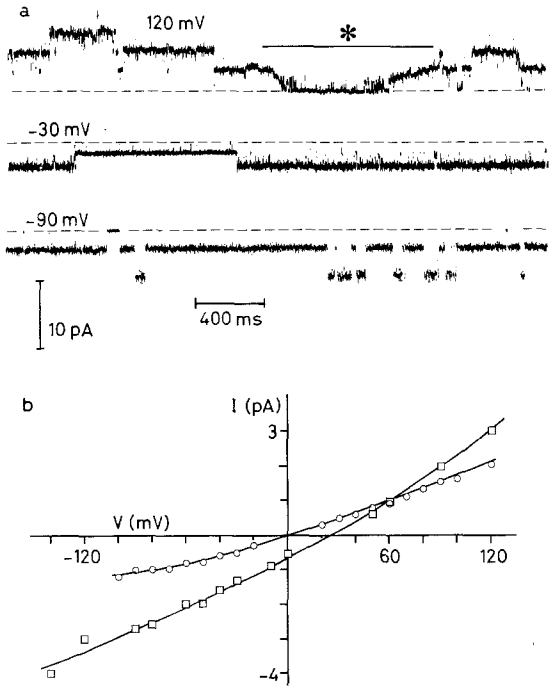

Fig. 13. Current traces and current-voltage relationships of the small Cl^- channel. (*a*) Current traces at 120, −30 and −90 mV. The pipette solution contained 150 mM NaCl, 5 mM HEPES and 4 mM EGTA; pH was adjusted to 7.2 with Tris; free Ca^{2+} was 3 μM. The bath solution contained 450 mM NaCl, 5 mM HEPES and 4 mM EGTA; pH was adjusted to 7.2 with Tris; free Ca^{2+} was 1 nM. In the traces at −30 and −90 mV, current steps of two different amplitudes can be recognized. The larger current steps correspond to the intermediate Cl^- channel; the smaller steps correspond to the small Cl^- channel. The current steps at 120 mV represent only those through the small Cl^- channel. The subconductance states are indicated by a horizontal bar with an asterisk. The traces were filtered at 900 Hz (−3 dB). (*b*) Current-voltage relationships obtained with symmetrical 150 mM NaCl solutions and solutions giving a threefold NaCl gradient. The pipette solution contained 150 mM NaCl, 5 mM HEPES and 4 mM EGTA; pH was adjusted to 7.2 with Tris; free Ca^{2+} was 1 nM to 3 μM. The bath solution contained: 150 mM NaCl (○) (n = 35) or 450 mM NaCl (□) (n = 2), 5 mM HEPES, pH adjusted to 7.2 with Tris, 4 mM EGTA; free Ca^{2+} was 1 nM to 30 μM. Standard errors of the mean are not shown because they are smaller than the symbol

From the shift in reversal potential of 24 mV with 450 mM NaCl in the bath, we calculate that the small Cl^- channel was more permeable to Cl^- than Na^+ by a factor of 15.6. The small Cl^- channel was insensitive to intracellular Ca^{2+}. Effect of DIDS was not examined for the small Cl^- channel.

Activated U937

U937 cells activated by rIFNγ ($n > 80$), rIFNαA ($n > 40$) or TPA ($n > 40$) were studied in the same way as the unstimulated cells. All four channels described above were observed in inside-out patches without any particular changes in the channel properties. The latency to first appearance of the Cl^- channels was similar.

Discussion

K^+ Channel

The K^+ channel of U937 is a Ca^{2+}-activated K^+ channel with small conductance (SK channel) that shows inward-rectification and is relatively voltage independent. Similar channels have been described in red blood cells [18], skeletal muscle [4], HeLa cells [38], an anterior pituitary cell line [27], renal epithelioid cells [12], aortic endothelial cells [37], and human B lymphocytes [28]. Recently Gallin has described a Ca^{2+}-activated inwardly rectifying K^+ channel in cultured human macrophages [15]. This macrophage K^+ channel had a conductance of 37 pS, which was slightly larger than that of the K^+ channel described here (28 pS). The difference is not due to the voltage range over which this rectifying conductance was measured. Our K^+ channel varied only from 28 to 31 pS over the entire voltage range of −100 to −180 mV. In human

monocytes and mouse macrophages, a classical inward-rectifying K^+ channel with 29-pS slope conductance has also been reported [16, 30]. However, the open probability of the K^+ channels in the literature was insensitive to Ca^{2+}, voltage dependent, and their outward current was never observed. Thus the channels differ from the present K^+ channel.

The inward-rectifying Ca^{2+}-activated K^+ channel differs from the large conductance Ca^{2+}-activated K^+ channel (BK channel, [1, 35]) that is present in human monocytes [14, 16, 29] and human alveolar macrophages (our observation). In circulating monocytes, the BK channel is absent, but is expressed after culture for several days [16]. In alveolar macrophages, such culture was not necessary to observe the channel (our observation). The observations that U937, a promonocyte [42], does not have BK channel and that the alveolar macrophage, a mature cell, has a BK channel lead to a speculation that the BK channel is expressed after differentiation. However, activation of U937 with rIFNγ, rIFNαA or TPA did not cause expression of the BK channel. Therefore, U937 cells differ from monocytes/macrophages in the expression of the BK channel.

A delayed outward-rectifying K^+ channel has been reported in mouse macrophages [17, 24, 36, 50] and U937 cells [39]. Our failure to detect this channel does not imply the absence of the channel because it may not be observed in inside-out patches [5]. Another type of K^+ channel has also been reported in U937 cells by McCann et al. [29]. The channel was observed only with positive potentials, was voltage dependent and Ca^{2+} insensitive. The channel is, thus, different from the K^+ channel in the present study.

Cl^- Channels

In monocytes/macrophages, only one kind of Cl^- channel, which is similar to the large Cl^- channel in the present study, has been reported [24, 36, 41]. The channel was observed mainly in inside-out patches and only occasionally in cell-attached patches. Our finding that the Cl^- channel had a latent period before being observed agrees with the previous studies and suggests existence of some factor(s) inhibitory to the channel *in situ*. The large Cl^- channel we describe also shares another prominent characteristic with other Cl^- channels: frequent appearance of subconductance states [11, 24, 26, 36, 41]. Excess filtering of the current record revealed six levels of the apparent subconductance states. If the increased noise level in the original current traces was due to rapid fluctuation between two specific subconductance states, the current level revealed with the filtering would be determined by the ratio of durations of the open and shut intervals. The number of such kinetic states might be multiple, as well as the number of subconductance levels. Relative stability of both the combination of subconductance levels and kinetics might result in a current trace as shown in Fig. 10*b,iii,* and instability of either might result in a current trace as shown in Fig. 10*b,ii.* The possibility of contamination by the intermediate and the small Cl^- channels should be considered as well. Amplitude of the apparent subconductance steps in the large Cl^- channel was similar to the single-channel amplitude of the intermediate Cl^- channel under similar experimental conditions. However, the absence of current steps superimposed on the fully open state of the large Cl^- channel makes this possibility unlikely.

The intermediate and the small Cl^- channels in the present study have not been described in monocytes/macrophages. They had characteristics partially similar to Cl^- channels in other preparations. The intermediate Cl^- channel most resembled the slow Cl^- channel in rat skeletal muscle [2]. The mean open time of both channels was tens of milliseconds. Both channels were voltage dependent. However, the voltage dependence of the Cl^- channel in rat skeletal muscle at positive potentials was not examined and cannot be compared. Neither channel could be observed in cell-attached patches, and neither was sensitive to intracellular Ca^{2+}. The intermediate Cl^- channel occasionally showed moding behavior; mean open time was shifted from tens of milliseconds to a few milliseconds or less. This moding behavior made the intermediate Cl^- channel like the fast Cl^- channel in rat skeletal muscle [2]. However, the skeletal muscle fast Cl^- channel and the intermediate U937 Cl^- channel differed in other ways. The skeletal muscle fast channel was active in cell-attached patches, while the U937 Cl^- channel was not. While the skeletal muscle fast Cl^- channel was inhibited by low pH, the U937 Cl^- channel was not affected by intracellular pH. The U937 channel had a smaller permeability ratio of Cl^- to Na^+ than the skeletal muscle channel, although the ratios of both were smaller than those of Cl^- channels in heart [10], and lymphocytes [8]. Permeability to $CH_3SO_4^-$ also differed; in the skeletal muscle Cl^- channels [2], current was decreased to near noise level when Cl^- was replaced by $CH_3SO_4^-$; in the intermediate U937 Cl^- channel, the current with $CH_3SO_4^-$ was 0.7 times as large as that with Cl^-. Chloride channels in human airway epithelium resemble both the intermediate and small

Cl^- channels in their *I-V* relationships and bursting appearance [13, 45]; however, the epithelial channels are more Cl^- selective and voltage independent.

Apparent subconductance states of the intermediate Cl^- channel were almost always accompanied by rapid openings and closings. Although they are possibly due to occurrence of another mode too rapid to be resolved with normal conductance, we cannot exclude the existence of subconductance states.

Anionic buffers such as HEPES have been reported to block Cl^- channels and make them polymers of many elementary channels in *Drosophila* neurons [48]. In the present study, however, anionic buffers, HEPES, BES, TES and EGTA, as well as a cationic buffer, Tris, had no effect on the kinetics or occurrence of the subconductance states of all the Cl^- channels. Thus, these buffers can be used in U937 experiments without deleterious effect. However, $CH_3SO_4^-$ cannot be used as an impermeant anion.

Cellular Activation

We could not detect any change in characteristics of ionic channels in inside-out patches from U937 cells after treatment with rIFNγ, rIFNαA or TPA. Thus, from our observations, ionic channels are not functional markers of U937 activation, at least as measured in excised patches. Other changes might be detected in outside-out patches or with the whole-cell configuration.

Another approach to studying roles of ionic channels in monocytes/macrophages would be to carry out experiments on intracellular vesicles. Chloride channels in other preparations have been proposed to participate in pH regulation in endosomes [46, 47] and Ca^{2+}-uptake in endoplasmic reticulum [23, 40]. Because receptor-recycling [7] and intracellular Ca^{2+} stores [21] have been shown to be important in monocytes/macrophages, the presence of Cl^- channels in such intracellular vesicles should be examined.

We would like to thank Dr. Leslie C. McKinney for critically reviewing the manuscript, and Dr. Hidetada Sasaki for helpful discussions.

References

1. Barrett, J.N., Magleby, K.L., Pallotta, B.S. 1982. Properties of single calcium-activated potassium channels in cultured rat muscle. *J. Physiol. (London)* **331:**211–230
2. Blatz, A.L., Magleby, K.L. 1985. Single chloride-selective channels active at resting membrane potentials in cultured rat skeletal muscle. *Biophys. J.* **47:**119–123
3. Blatz, A.L., Magleby, K.L. 1986. Quantitative description of three modes of activity of fast chloride channels from rat skeletal muscle. *J. Physiol. (London)* **378:**141–174
4. Blatz, A.L., Magleby, K.L. 1986. Single apamin-blocked Ca-activated K^+ channels of small conductance in cultured rat skeletal muscle. *Nature (London)* **323:**718–720
5. Bregestovski, P., Redkozubov, A., Alexeev, A. 1986. Elevation of intracellular calcium reduces voltage-dependent potassium conductance in human T cells. *Nature (London)* **319:**776–778
6. Buisman, H.P., Steinberg, T.H., Fischbarg, J., Silverstein, S.C., Vogelzang, S.A., Ince, C., Ypey, D.L., Leijh, P.C.J. 1988. Extracellular ATP induces a large nonselective conductance in macrophage plasma membranes. *Proc. Natl. Acad. Sci. USA* **85:**7988–7992
7. Celada, A., Allen, R., Esparza, I., Gray, P.W., Schreiber, R.D. 1985. Demonstration and partial characterization of the interferon-gamma receptor on human mononuclear phagocytes. *J. Clin. Invest.* **76:**2196–2205
8. Chen, J.H., Schulman, H., Gardner, P. 1989. A cAMP-regulated chloride channel in lymphocytes that is affected in cystic fibrosis. *Science* **243:**657–660
9. Colquhoun, D., Sigworth, F.J. 1983. Fitting and statistical analysis of single-channel records. *In:* Single-Channel Recording. B. Sakmann and E. Neher, editors. pp. 191–263. Plenum, New York
10. Coronado, R., Latorre, R. 1982. Detection of K^+ and Cl^- channels from calf cardiac sarcolemma in planar lipid bilayer membranes. *Nature (London)* **298:**849–852
11. Fox, J.A. 1987. Ion channel subconductance states. *J. Membrane Biol.* **97:**1–8
12. Friedrich, F., Paulmichl, M., Kolb, H.-A., Lang, F. 1988. Inward rectifier K channels in renal epithelioid cells (MDCK) activated by serotonin. *J. Membrane Biol.* **106:**149–155
13. Frizzell, R.A., Rechkemmer, G., Shoemaker, R.L. 1986. Altered regulation of airway epithelial cell chloride channels in cystic fibrosis. *Science* **233:**558–560
14. Gallin, E.K. 1984. Calcium- and voltage-activated potassium channels in human macrophages. *Biophys. J.* **46:**821–825
15. Gallin, E.K. 1989. Evidence for a Ca-activated inwardly rectifying K channel in human macrophages. *Am. J. Physiol.* **257:**C77–C85
16. Gallin, E.K., McKinney, L.C. 1988. Patch-clamp studies in human macrophages: Single-channel and whole-cell characterization of two K^+ conductances. *J. Membrane Biol.* **103:**55–66
17. Gallin, E.K., Sheehy, P.A. 1985. Differential expression of inward and outward potassium currents in the macrophage-like cell line J774.1. *J. Physiol. (London)* **369:**475–499
18. Grygorczyk, R., Schwarz, W., Passow, H. 1984. Ca^{2+}-activated K^+ channels in human red cells. Comparison of single-channel currents with ion fluxes. *Biophys. J.* **45:**693–698
19. Hamill, O.P., Marty, A., Neher, E., Sakmann, B., Sigworth, F.J. 1981. Improved patch-clamp techniques for high-resolution current recording from cells and cell-free membrane patches. *Pfluegers Arch.* **391:**85–100
20. Harafuji, H., Ogawa, Y. 1980. Re-examination of the apparent binding constant of ethylene glycol *bis*(β-aminoethyl ether)-N,N,N′,N′-tetraacetic acid with calcium around neutral pH. *J. Biochem. (Tokyo)* **87:**1305–1312

21. Hirata, M., Suematsu, E., Hashimoto, T., Hamachi, T., Koga, T. 1984. Release of Ca^{2+} from a non-mitochondrial store site in peritoneal macrophages treated with saponin by inositol 1,4,5-trisphosphate. *Biochem. J.* **223:**229–236
22. Kanno, T., Sasaki, H., Takishima, T. 1987. Chloride channels in human macrophage. *Biophys. J.* **51:**254*a*
23. Kemmer, T.P., Bayerdörffer, E., Will, H., Schulz, I. 1987. Anion dependence of Ca^{2+} transport and (Ca^{2+} + K^+)-stimulated Mg^{2+}-dependent transport ATPase in rat pancreatic endoplasmic reticulum. *J. Biol. Chem.* **262:**13758–13764
24. Kolb, H.-A., Ubl, J. 1987. Activation of anion channels by zymosan particles in membranes of peritoneal macrophages. *Biochim. Biophys. Acta* **899:**239–246
25. Koren, H.S., Anderson, S.J., Larrick, J.W. 1979. In vitro activation of a human macrophage-like cell line. *Nature (London)* **279:**328–331
26. Krouse, M.E., Schneider, G.T., Gage, P.W. 1986. A large anion-selective channel has seven conductance levels. *Nature (London)* **319:**58–60
27. Lang, D.G., Ritchie, A.K. 1987. Large and small conductance calcium-activated potassium channels in the GH_3 anterior pituitary cell line. *Pfluegers Arch.* **410:**614–622
28. Mahaut-Smith, M.P., Schlichter, L.C. 1989. Ca^{2+}-activated K^+ channels in human B lymphocytes and rat thymocytes. *J. Physiol. (London)* **415:**69–83
29. McCann, F.V., Keller, T.M., Guyre, P.M. 1987. Ion channels in human macrophages compared with the U-937 cell line. *J. Membrane Biol.* **96:**57–64
30. McKinney, L.C., Gallin, E.K. 1988. Inwardly rectifying whole-cell and single-channel K currents in the murine macrophage cell line J774.1. *J. Membrane Biol.* **103:**41–53
31. McManus, O.B., Magleby, K.L. 1988. Kinetic states and modes of single large-conductance calcium-activated potassium channels in cultured rat skeletal muscle. *J. Physiol. (London)* **402:**79–120
32. Nelson, D.J., Jacobs, E.R., Tang, J.M., Zeller, J.M., Bone, R.C. 1985. Immunoglobulin G-induced single ionic channels in human alveolar macrophage membranes. *J. Clin. Invest.* **76:**500–507
33. Nilsson, K., Forsbeck, K., Gidlund, M., Sundström, C., Tötterman, T., Sällström, J., Venge, P. 1981. Surface characteristics of the U-937 human histiocytic lymphoma cell line: Specific changes during inducible morphologic and functional differentiation in vitro. *Haematol. Blood Transf.* **26:**215–221
34. Palacios, R., Ivhed, I., Sideras, P., Nilsson, K., Sugawara, I., Fernandez, C. 1982. Accessory function of human tumor cell lines: I. Production of interleukin 1 by the human histiocytic lymphoma cell line U-937. *Eur. J. Immunol.* **12:**895–899
35. Petersen, O.H., Maruyama, Y. 1984. Calcium-activated potassium channels and their role in secretion. *Nature (London)* **307:**693–696
36. Randriamampita, C., Trautmann, A. 1987. Ionic channels in murine macrophages. *J. Cell Biol.* **105:**761–769
37. Sauve, R., Parent, L., Simoneau, C., Roy, G. 1988. External ATP triggers a biphasic activation process of a calcium-dependent K^+ channel in cultured bovine aortic endothelial cells. *Pfluegers Arch.* **412:**469–481
38. Sauvé, R., Simoneau, C., Monette, R., Roy, G. 1986. Single-channel analysis of the potassium permeability in HeLa cancer cells: Evidence for a calcium-activated potassium channel of small unitary conductance. *J. Membrane Biol.* **92:**269–282
39. Schlichter, L., Sidell, N., Hagiwara, S. 1986. Potassium channels mediate killing by human natural killer cells. *Proc. Natl. Acad. Sci. USA* **83:**451–455
40. Schmid, A., Gögelein, H., Kemmer, T.P., Schulz, I. 1988. Anion channels in giant liposomes made of endoplasmic reticulum vesicles from rat exocrine pancreas. *J. Membrane Biol.* **104:**275–282
41. Schwarze, W., Kolb, H.-A. 1984. Voltage-dependent kinetics of an anionic channel of large unit conductance in macrophages and myotube membranes. *Pfluegers Arch.* **402:**281–291
42. Sundström, C., Nilsson, K. 1976. Establishment and characterization of a human histiocytic lymphoma cell line (U-937). *Int. J. Cancer* **17:**565–577
43. Unanue, E.R. 1989. Macrophages, antigen-presenting cells, and the phenomena of antigen handling and presentation. *In:* Fundamental Immunology. (2nd Ed.) W.E. Paul, editor. pp. 95–115. Raven, New York
44. Virelizier, J., Perez, N., Arenzana-Seisdedos, F., Devos, R. 1984. Pure interferon gamma enhances class II HLA antigens on human monocyte cell lines. *Eur. J. Immunol.* **14:**106–108
45. Welsh, M.J. 1986. An apical-membrane chloride channel in human tracheal epithelium. *Science* **232:**1648–1650
46. Wileman, T., Boshans, R., Stahl, P. 1985. Uptake and transport of mannosylated ligands by alveolar macrophages. Studies of ATP-dependent receptor-ligand dissociation. *J. Biol. Chem.* **260:**7387–7393
47. Wileman, T., Harding, C., Stahl, P. 1985. Receptor-mediated endocytosis. *Biochem. J.* **232:**1–14
48. Yamamoto, D., Suzuki, N. 1987. Blockage of chloride channels by HEPES buffer. *Proc. R. Soc. London B* **230:**93–100
49. Young, J.D.-E., Unkeless, J.C., Young, T.M., Mauro, A., Cohn, Z.A. 1983. Role for mouse macrophage IgG Fc receptor as ligand-dependent ion channel. *Nature (London)* **306:**186–189
50. Ypey, D.L., Clapham, D.E. 1984. Development of a delayed outward-rectifying K^+ conductance in cultured mouse peritoneal macrophages. *Proc. Natl. Acad. Sci. USA* **81:**3083–3087

Received 19 October 1989; revised 22 January 1990